Fermi National Accelerator Laboratory

FERMILAB-FN-659

Instabilities and Space-Charge Effects of the High-Intensity Proton Driver

King-Yuen Ng and Zubao Qian

Fermi National Accelerator Laboratory
P.O. Box 500, Batavia, Illinois 60510

July 1997

Operated by Universities Research Association Inc. under Contract No. DE-AC02-76CH03000 with the United States Department of Energy

FN-659

INSTABILITIES AND SPACE-CHARGE EFFECTS OF THE HIGH-INTENSITY PROTON DRIVER

King-Yuen Ng and Zubao Qian

Fermi National Accelerator Laboratory, P.O. Box 500, Batavia, IL 60510*

(July, 1997)

Abstract

Microwave instabilities are studied for the two-ring proton driver destined for the muon collider. Because of the operation at the high intensity of 1×10^{14} particles in each rings, space-charge effects are important. In the first ring, the distortion of the rf wave-form is severe and ferrite insertion is suggested to cancel the space-charge effect. In order to control the inductance of the ferrite during ramping, transverse biasing of the ferrite is proposed.

*Operated by the Universities Research Association, Inc., under contract with the U.S. Department of Energy.

I. INTRODUCTION

In order to supply enough muons to the 250-250 GeV muon collider with a luminosity of 5×10^{33} cm^{-2}s^{-1} for the performance of meaningful experiments, a high-intensity proton driver will be required to provide for the necessary amount of protons for the production of pions which subsequently decay into muons. This proton driver should deliver 2 bunches of protons, 5.0×10^{13} each, at 16 GeV with an rms length of ~ 1 ns and at a repetition rate of 15 Hz [1]. Proton bunches of such high intensity will be subjected to severe space-charge effects. To lower the Laslett tune shift, we would like the injected beam from the linac to have a high energy of 1 GeV and a large 95% normalized emittance of 200 π mm-mr [2]. For economical reason, the proton driver is divided into 2 rings. The lower-energy ring accelerates protons from kinetic energy 1 to 4.5 GeV, has an rf harmonic of 2, a very large aperture, and a circumference as small as possible. The higher-energy ring accelerates protons of shorter bunch lengths from kinetic energy 4.5 GeV to 16 GeV, has a shorter rf wavelength and a smaller aperture. A bunch rotation is performed to obtain a shorter bunch length just before the extraction. Thus two such bunch rotations can be performed with the two-ring system. Some designed parameters provided by Ankenbrandt for the two rings at injection are listed in Table I [2]. Unless stated otherwise, our discussions are at injection when the space-charge effects are most important. We start from a simple analysis of the incoherent Laslett tune shift in Sec. II and microwave instabilities in Sec. III. The modification of the rf wave form by the coherent space-charge force will be computed in Sec. IV. To compensate this modification, we suggest in Sec. V to use an insertion of a hollow ferrite cylinder in the beam pipe. The transverse force of the ferrite insertion and the dielectric constant of the ferrite are also discussed. To control the inductance of the insertion and minimize loss, perpendicular biasing is proposed in Sec. VI. Finally, the conclusion is given in Sec. VII.

II. LASLETT TUNE SHIFTS

Laslett tune shifts at injection are given by [3]

$$\Delta\nu = -\frac{3N_{\rm total}r_p}{2\gamma^2\beta\epsilon_{\rm N95}B} = \begin{cases} -0.393 & \text{1st ring} \\ -0.389 & \text{2nd ring}\,, \end{cases} \tag{2.1}$$

Table I: Designed parameters for the low-energy ring.

	First Ring	Second Ring
Kinetic Energy (GeV)	1.0	4.5
Relativistic gamma γ	2.0658	5.7960
Relativistic beta β	0.8750	0.9850
Cycling rate (Hz)	15	15
Circumference, C (m)	180.649	474.365
Number of bunches M	2	2
Number per bunch, N_b	5.0×10^{13}	5.0×10^{13}
Bucket bunching factor, B	0.25	0.25
Transition γ_t	7	25
95% bunch area, A (eV-s)	1.0	1.0
95% normalized emittance, $\epsilon_{\rm N95}$ (π-m)	200×10^{-6}	240×10^{-6}

where r_p is the classical proton radius and N_b is number of protons per bunch, h the rf harmonic, $\epsilon_{\rm N95}$ the 95% normalized emittance, and B the bucket bunching factor, which is the ratio of the mean linear charge density in one occupied bucket to the maximum linear charge density. The formula of Laslett tune shift may be a naive model because the actual tune shift due to space charge depends critically on the bunch distribution [4]. Nevertheless, the Laslett tune shift does give a useful guideline in the design of particle accelerators. Experience at Fermilab [5], Brookhaven [6], and elsewhere tells us that a machine with all stop bands minimized should be able to operate at a Laslett tune depression of not more than 0.4. This has been the criterion with which the two rings are designed and the injection energy of the second ring is chosen [2].

III. MICROWAVE INSTABILITIES

The average beam currents at injection are, respectively, $I_{\rm av}=eMN_bf_0=23.26$ and 9.974 Amp for the two rings, where $f_0=\omega_0/(2\pi)=1.452$ and 0.623 MHz are the respective revolution frequencies, $M=2$ is the number of bunches in each ring, and e the proton charge. With a bucket bunching factor of $B=0.25$, the peak currents become $I_{\rm pk}=93.06$ and 418.90 Amp for the two rings. For a parabolic bunch, the linear distribution for particles at time τ ahead of the synchronous particle is

$$\lambda(\tau) = \frac{3eN_b}{4\hat{\tau}}\left(1 - \frac{\tau^2}{\hat{\tau}^2}\right) \, . \tag{3.1}$$

The half bunch lengths are therefore $\hat{\tau} = 64.56$ and 14.34 ns for the two rings. The time advance τ is a more convenient variable here than the distance $z = \beta c\tau$ along the ring because the velocities of the beam particles are significantly less than c, the velocity of light. The linear half lengths of the bunches in the two rings can then be derived and are, respectively, $\hat{\ell} = 16.94$ and 4.24 m. For a bunch area of 1 eV-s, the half energy spreads are, respectively, $\widehat{\Delta E}/E = 2.544 \times 10^{-3}$ and 4.081×10^{-3}, while the half momentum spreads are $\hat{\delta} = 3.222 \times 10^{-3}$ and 4.206×10^{-3}. We assume an average betatron amplitude of $\langle\beta\rangle = 25$ m and an average dispersion function of $\langle D\rangle = 1.8$ m. The average beam radius is then

$$a \approx \sqrt{\frac{\epsilon_{\rm N95}\langle\beta\rangle}{\gamma\beta} + \left(\langle D\rangle\hat{\delta}\right)^2} = \begin{cases} 5.29 \text{ cm} & \text{1st ring} \\ 3.33 \text{ cm} & \text{2nd ring}\,. \end{cases} \tag{3.2}$$

It is very probable that a beam pipe or vacuum chamber of radius $b = 8$ cm will be required for the first ring and one with $b = 5$ cm for the second ring, because the losses in rings with such high intensities should be minimized to less than 0.1%. The longitudinal space-charge impedances of the beam are then

$$\left.\frac{Z_0^\parallel}{n}\right|_{\rm spch} = i\frac{Z_0}{2\gamma^2\beta}\left(1 + 2\ln\frac{b}{a}\right) = \begin{cases} 92.1 \text{ Ohms} & \text{1st ring} \\ 10.3 \text{ Ohms} & \text{2nd ring}\,, \end{cases} \tag{3.3}$$

where $Z_0 \approx 377$ Ohms is the free-space impedance. The limits of microwave instability driven by a broad-band impedance are given by the Boussard-modified Keil-Schnell criterion [7]:

$$\left|\frac{Z_0^\parallel}{n}\right| < F_\parallel \frac{E|\eta|}{e\beta^2 I_{\rm pk}}\left(\frac{\Delta E}{E}\right)^2_{\rm FWHM} = \begin{cases} 75.3 \text{ Ohms} & \text{1st ring} \\ 12.5 \text{ Ohms} & \text{2nd ring}\,, \end{cases} \tag{3.4}$$

where the form factor $F_\parallel \approx 1$ for a parabolic bunch, η is the slippage factor, and the full-width-at-half-maximum energy spread is $(\Delta E/E)_{\rm FWHM} = \sqrt{2}(\widehat{\Delta E}/E)$. Different interpretation of these limits can lead to different stability result. Since both the low-energy and high-energy rings operate below transition, one may think that microwave instability cannot be driven by the space-charge force. However, if we take the parabolic distribution seriously, the bunch will be unstable even with the present of any small resistive impedance. This is because the discontinuous slope of the parabolic distribution at the two edges of the momentum spread will shrink the space-charge side of the stability curve to zero, as depicted in Fig. 1(a). However, such a distribution is not physical. Any momentum distribution with a slope continuous at the edges of the distribution will enhance the space-charge side of the stability curve instead, as depicted in Fig. 1(b). If the momentum distribution has an infinite smooth tail like the Gaussian distribution, the stability curve on the capacitive side will extend to infinity as shown in Fig. 1(c). Hofmann [8] showed by simulation that a momentum-spread tail would develop at the early stage of the instability. This tail changed the shape of the stability curve leading to a nonlinear saturation of the instability. Thus, the Boussard-modified Keil-Schnell limit is usually too pessimistic and the actual stability limit driven by space-charge is usually a few times the Keil-Schnell value. Since our computed Keil-Schnell limits are roughly of the same order as the space-charge impedances, it may be safe to conclude that longitudinal microwave instability would not happen for the two rings.

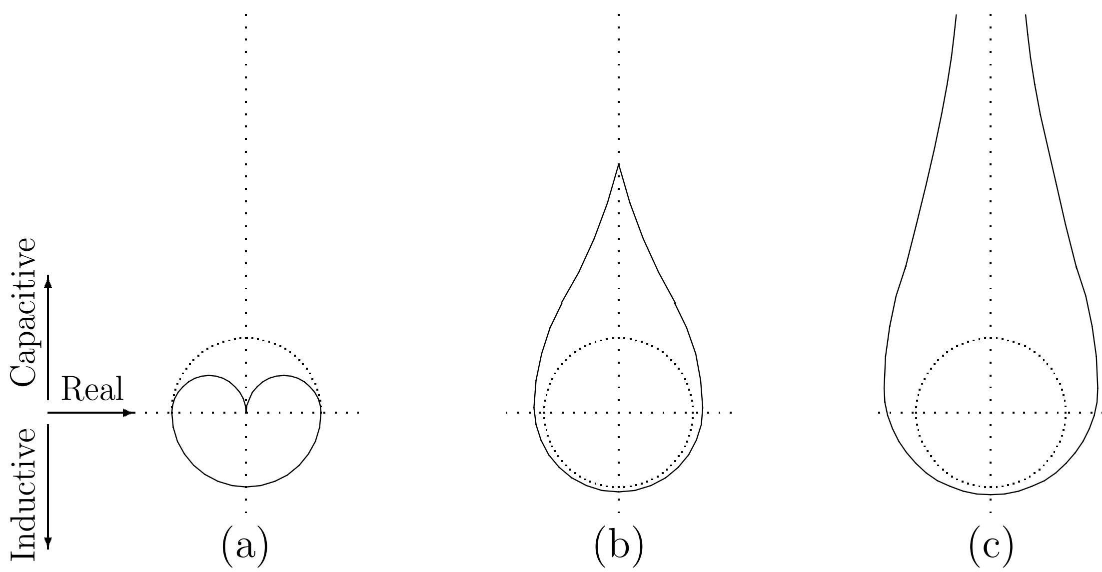

Fig. 1: Schematic drawings for the longitudinal microwave stability curves below transition for (a) momentum distribution that has a slope discontinuous at the ends of the spread like the parabolic or cosine distribution, (b) momentum distribution with a smooth slope at the ends of the distribution like $(1-x^2)^n$ where $n>1$, and (c) momentum distribution with infinite smooth tails like the Gaussian distribution. The Keil-Schnell limit is plotted as dotted circles. The abscissa is the real part of the longitudinal impedance and the ordinate the imaginary part.

For adiabatic ramping, the Keil-Schnell limit is proportional to $\hat{\Delta E}/E$. As energy increases $\hat{\Delta E}$ increases while E^{-1} decreases as γ^{-1}. However, the space charge impedance is proportional to $\gamma^2\beta$. Therefore, the bunches will be more stable as energy increases.

A broad-band transverse impedance will also drive the transverse microwave instability. Here, again the most important coupling transverse impedance comes from the space-charge force, which gives the contribution

$$Z_1^\perp|_{\rm spch} = i\frac{RZ_0}{\beta^2\gamma^2}\left(\frac{1}{a^2}-\frac{1}{b^2}\right) = \begin{cases} 0.665 \text{ MOhms/m} & \text{1st ring} \\ 0.438 \text{ MOhms/m} & \text{2nd ring}\,, \end{cases} \tag{3.5}$$

where R is the average radius of either ring. Similar to the Boussard-modified Keil-Schnell limit, the limit for transverse microwave instability driven by a broad-band impedance centered at the revolution harmonic n is

$$|Z_1^\perp| < F_\perp \frac{4\nu\beta}{eRI_{\rm pk}}\left(\Delta E\right)_{\rm FWHM}|(n-\nu)\eta+\nu\xi|\;, \tag{3.6}$$

where the form factor $F_\perp \approx 1$ for a parabolic distribution, and ξ is the chromaticity. We use the cutoff harmonics of the beam pipes or vacuum chambers, $n_{\text{cut off}} = 2.405c/(2\pi b) = 987.8$ and 3687, as the central frequencies of the driving impedances and $\nu \approx 2.2$ and ~ 12 as the betatron tune. Then we obtain the limit $|Z_1^\perp| < 4.24$ and 4.87 MOhms/m, which are much larger than the respective space-charge values. Thus, transverse microwave instability should not pose any problem here, especially when both rings operate below transition.

IV. POTENTIAL-WELL DISTORTION

Knowing the bunch lengths and the momentum spreads, the synchrotron tunes can be computed easily,

$$\nu_s = \frac{|\eta|\hat\delta}{\omega_0\hat\tau} = \begin{cases} 0.001207 & \text{1st ring} \\ 0.002112 & \text{2nd ring}\,. \end{cases} \tag{4.1}$$

Without the consideration of the forces due to space charge and any other impedance, the required rf voltages required to set up the buckets to fit the bunches are

$$V_{\rm rf} = \frac{2\pi\beta^2E\nu_s^2}{|\eta|h} = \begin{cases} 31.73 \text{ kV} & \text{1st ring} \\ 249.96 \text{ kV} & \text{2nd ring}\,. \end{cases} \tag{4.2}$$

The rf voltages seen by particle at a time advance τ from the bunch centers are

$$V_{\rm rf}\sin(-h\omega_0\tau)\approx -V_{\rm rf}\left(\frac{3\pi B}{2}\right)\left(\frac{\tau}{\hat\tau}\right)=\left\{\begin{array}{ll} -7.38\left(\dfrac{\tau}{\hat\tau}\right)\ \text{kV} & \text{1st ring}\\[2ex] -\,94.48\left(\dfrac{\tau}{\hat\tau}\right)\ \text{kV} & \text{2nd ring}\,,\end{array}\right. \tag{4.3}$$

where $B=0.25$ is the bunching factor, $\hat\ell$ is the half bunch length, the sinusoidal rf has been linearized, and the parabolic longitudinal distribution has been assumed. The negative signs in Eq. (4.3) signify that the synchronous phase or stable fixed point is zero for operation below transition.

However, in our situation of low energy and high intensity, the space-charge force shaping the bunch distribution is large and dominates over that due to other coupling impedance. A particle at time advance τ from bunch center sees a longitudinal electric space-charge field

$$E_{z\,\rm spch}=-\frac{eZ_0}{4\pi\beta^2\gamma^2c}\left(1+2\ln\frac{b}{a}\right)\frac{d\lambda}{d\tau}\,, \tag{4.4}$$

where $\lambda(\tau)$ is the linear density of the bunch which, for a parabolic distribution, is given by Eq. (3.1). The voltage seen per turn is $V_{\rm spch}=E_{s\,\rm spch}\,C$, which can be written as

$$V_{\rm spch}=\frac{3\pi I_b}{(\omega_0\hat\tau)^2}\left|\frac{Z_0^\parallel}{n}\right|_{\rm spch}\left(\frac{\tau}{\hat\tau}\right)\,, \tag{4.5}$$

which gives 29.1 kV at the either end of the bunch for the first ring and 14.7 kV for the second ring. Here, $I_b=I_{\rm av}/M$ is the average current per bunch Comparing Eqs.(4.3) and (4.5), we see that the space-charge distortion of the rf force will be small for the second ring but very large for the first ring. Thus, the rf voltage at injection must be increased to $V_{\rm rf}=56.42$ kV for the first ring in order to cancel the effect of space charge. Another possibility to cope with this space-charge force is to compensate it by using a ferrite insert in the vacuum chamber, which we will study in the next section.

V. FERRITE COMPENSATION

V.1 INDUCTANCE INSERTION

From Eq. (4.5), we see that the effect of the space-charge force on the rf potential can be minimized if the space-charge impedance is canceled by adding an inductance.

If a hollow cylinder of ferrite of length L, inner and outer radii b and d is encircling the beam, an inductive impedance

$$\left.\frac{Z_0^{\parallel}}{n}\right|_{\rm ind} = -i\frac{Z_0\omega_0}{2\pi c}\mu L \,\ln\frac{d}{b}\,, \tag{5.1}$$

will be introduced, where μ is the relative permeability of the ferrite. Here, we discuss this ferrite insertion for the first ring only because the space-charge distortion of the rf is small for the second ring. For example, with $\mu = 1000$, $b = 8.0$ cm, and $d = 8.8$ cm, a length of $L = 52.96$ cm will be enough to cancel a space-charge impedance of $|Z_0^{\parallel}/n|_{\rm spch} = 92.1$ Ohms for the first ring at injection.

V.2 LOSSES

Unfortunately, ferrite of high permeability is often accompanied by high resistive losses. A conventional way to introduce loss is to replace the relative magnetic permeability by $\mu \to \mu' - i\mu''$. However, with μ' and μ'' frequency independent even at low frequencies, the expression

$$\left.Z_0^{\parallel}(\omega)\right|_{\rm ferrite} = (\mu'' - i\mu')\frac{Z_0\omega}{2\pi c}L \,\ln\frac{d}{b}\,, \tag{5.2}$$

is not a valid impedance, since it violates causality and does not satisfy Hilbert's transform. Noticing that μ' is mostly a constant at low frequencies and μ'' goes through a resonance at frequency $\omega_r/(2\pi)$, a better representation of the ferrite impedance is a broad-band resonance

$$\left.Z_0^{\parallel}(\omega)\right|_{\rm ferrite} = \frac{R_s}{1 - iQ\left(\dfrac{\omega}{\omega_r} - \dfrac{\omega_r}{\omega}\right)}\,, \tag{5.3}$$

where Q is the quality factor. Equating Eq. (5.3) at low frequencies with the inductive part of the ferrite impedance in Eq. (5.1), the shunt impedance R_s is given by

$$R_s = \frac{Q\omega_r}{\omega_0}\left|\frac{Z_0^{\parallel}}{n}\right|_{\rm ind} \tag{5.4}$$

The real part of the ferrite impedance is therefore

$$\mathcal{R}e\; \left.Z_0^{\parallel}(\omega)\right|_{\rm ferrite} = \frac{R_s}{1 + Q^2\left(\dfrac{\omega}{\omega_r} - \dfrac{\omega_r}{\omega}\right)^2} \;\xrightarrow[\text{low freq}]{}\; \frac{\omega^2}{Q\omega_r\omega_0}\left|\frac{Z_0^{\parallel}}{n}\right|_{\rm ind}\,. \tag{5.5}$$

At resonance,

$$\mathcal{R}e\, Z_0^{\parallel}(\omega)\Big|_{\rm ferrite} = R_s \equiv \frac{\omega_r\mu''}{\omega_0\mu'}\left|\frac{Z_0^{\parallel}}{n}\right|_{\rm ind} . \tag{5.6}$$

which gives the definition of μ''. Comparing Eqs. (5.4) and (5.6), we obtain

$$\mu'' = Q\mu' . \tag{5.7}$$

In this way μ' has been defined as the real part of the relative magnetic permeability at *low* frequencies, and μ'' the negative of the imaginary part at *resonant* frequency.

We are now in a position to compute the loss. For a bunch with spectrum

$$\tilde{\lambda}(\omega) = \frac{1}{2\pi}\int_{-\infty}^{\infty} d\tau\, \lambda(\tau)e^{-i\omega\tau} , \tag{5.8}$$

the energy *gained* per turn for a particle at time advance τ is

$$\Delta\mathcal{E}(\tau) = -e\int_z^{\infty} dz\, \lambda(z')W_0'(z-z') , \tag{5.9}$$

where $W_0'(z)$ is the longitudinal wake function, which is the Fourier transform of the ferrite impedance of Eq. (5.3). It vanishes when $\tau > 0$. For $\tau < 0$, it is given by

$$W_0'(\tau) = \frac{\omega_r R_s}{Q}\, e^{\alpha\tau}\left(\cos\bar{\omega}\tau + \frac{\alpha}{\bar{\omega}}\sin\bar{\omega}\tau\right) , \tag{5.10}$$

where the shifted resonant frequency is $\bar{\omega} = \sqrt{\omega_r^2 - \alpha^2}$. The e-folding length of the wake is $\alpha^{-1} = 2Q/\omega_r = 3.18$ ns which is very much shorter than the length of the bunch. We can therefore expand $\lambda(\tau')$ as a Taylor series about $\tau' = \tau$. The energy gained can then be computed exactly as

$$\Delta\mathcal{E}(\tau) = e\sum_{n=0}\lambda^{(n)}(\tau)\frac{R_s}{Q\bar{\omega}\omega_r^{n-1}}\sin n\theta , \tag{5.11}$$

where $\lambda^{(n)}(\tau)$ is the n-th derivative of λ with respective to τ, $\sin\theta = \bar{\omega}/\omega_r$ and $\cos\theta = \alpha/\omega_r$. For the parabolic distribution, there are only two terms. However, since the first derivative is discontinuous at the ends of the bunch, the expansion will fail over there. For particles that are not too close to the edges of the bunch, the loss per turn is

$$\Delta\mathcal{E}(\tau) = \frac{e}{\omega_0}\left|\frac{Z_0^{\parallel}}{n}\right|_{\rm ind}\left[\lambda'(\tau) + \frac{1}{Q\omega_r}\lambda''(\tau)\right] , \tag{5.12}$$

where the Eq. (5.4) has been used. Substituting Eq. (3.1), we obtain

$$\Delta\mathcal{E}(\tau) = -\frac{3e\pi I_b}{(\omega_0\hat{\tau})^2}\left|\frac{Z_0^{\parallel}}{n}\right|_{\rm ind}\left(\frac{\tau}{\hat{\tau}}\right) - \frac{3e\pi I_b}{Q\omega_r\omega_0^2\hat{\tau}^3}\left|\frac{Z_0^{\parallel}}{n}\right|_{\rm ind} . \tag{5.13}$$

The first term is the contribution of the inductance of the ferrite, which cancels the space-charge voltage of Eq. (3.3) if $|Z_0^{\parallel}/n|_{\rm ind}$ is chosen to equal to $|Z_0^{\parallel}/n|_{\rm spch}$. The second term gives the average loss of energy per particle per turn. When the space-charge force is canceled, this amount to 1.13 keV. The power loss is

$$P = \frac{3\pi I_b^2}{Q\omega_r\omega_0^2\hat{\tau}^3}\left|\frac{Z_0^{\parallel}}{n}\right|_{\rm ind} , \tag{5.14}$$

or 14.3 kw per bunch. The energy loss per particle is small. We note that the loss is inversely proportional to the third power of the bunch length. As the protons are ramped to higher energies, the bunches becomes shorter and shorter. For example, when the bunches are prepared for extraction into the second ring, the half bunch length will be 14.34 ns or 4.5 times shorter. However, the longitudinal space-charge impedance will be 8.862 times smaller. Thus the energy loss per particle will be increased 10.3 times to 11.6 keV. Also for a non-parabolic bunch, this energy will be position dependent along the bunch, making equal energy compensation impossible. For this reason, it will be best to reduce the ferrite loss to a minimum, which we shall study in Sec. VI.

V.3 FERRITE LOADED WAVEGUIDE

In the previous section, we studied the response of the ferrite insertion at low frequencies. We would like to study also the high-frequency response, the effect of the dielectric constant, and transverse effects. In this section, we look into a model of an infinite beam pipe of radius $r = d$ infinitely conductive, lined with ferrite in the radial region $b < r < d$. The loss is assumed to be small. For constant relative magnetic permeability μ and dielectric constant ϵ, the electromagnetic field left by a charged particle can be computed [10]. The transverse and longitudinal wakes of the m-th azimuthal over a distance L are

$$W_m(z) = \frac{Z_0cL}{2\pi m d^{2m+1}}\sum_{\lambda=1}^{\infty}\tilde{F}_{rm\lambda}(x_{m\lambda})\sin\frac{x_{m\lambda}z}{d\sqrt{\epsilon\mu-1}} \tag{5.15}$$

$$W'_m(z) = \frac{Z_0 cL}{2\pi(1+\delta_{0m})d^{2m+2}} \sum_{\lambda=1}^{\infty} \tilde{F}_{zm\lambda}(x_{m\lambda}) \cos \frac{x_{m\lambda} z}{d\sqrt{\epsilon\mu - 1}} \tag{5.16}$$

where $x_{m\lambda}$ is the λ-th zero of some combinations of modified Bessel functions of order m and $F_{rm\lambda}$ is the corresponding reduced wake force. The above formulas are just summations over sharp resonances.

When the ferrite layer is thin, there are analytic expressions. Take the monopole case of $m = 0$. Let t be the thickness of the ferrite layer. When $\delta = t/b \ll 1$, $x_{z01} = \sqrt{2\epsilon/\delta}$ and $\tilde{F}_{z01} = 4$. Then the resonant frequency is

$$\omega_{z01} = \frac{x_{z01} c}{d\sqrt{\epsilon\mu - 1}} = \frac{c}{d}\sqrt{\frac{2\epsilon}{\delta(\epsilon\mu - 1)}}\,. \tag{5.17}$$

Comparing Eq. (5.15) with Eq. (5.14), we obtain

$$\frac{R_s \omega_r}{Q} = \frac{Z_0 cL}{4\pi d^2} \hat{F}_{z01}(x_{z01})\,. \tag{5.18}$$

The impedance for a length L can be written down readily with the aid of Eq. (5.3). At low frequencies, it is given by

$$\frac{Z_0^{\|}}{n} = -i\frac{\omega_0 Z_0}{2\pi c}\left(\mu - \frac{1}{\epsilon}\right) L\delta\,. \tag{5.19}$$

This is exactly the same expression as Eq. (5.1) with the effect of the dielectric constant included. However, the dielectric constant contributes only negligibly when $\mu\epsilon \gg 1$. This is probably due to the fact that the capacitance between the beam and the surface of the ferrite and the capacitance between the surface of the ferrite and the beam-pipe wall add reciprocally, leading to negligible contribution of the latter capacitance. For the situation of $\mu = 1000$, $\delta = 0.1$, and $d = 8.8$ cm, the resonant frequency is $f_{01} = 76.7$ MHz. Note that this resonance is a result of the geometry of the waveguide and has nothing to do with the intrinsic resonance of the ferrite material discussed in the previous section. However, it is not good that this resonance is smaller than the intrinsic resonance of the ferrite, because the geometry of the waveguide will interfere with the properties of the ferrite. Therefore, it is advisable to use a ferrite with a lower permeability so that the resonances of the waveguide will be pushed to much higher frequencies.

For the dipole mode ($m = 1$), when the ferrite layer is thin, the zero of the combination of Bessel function x_{r11} is the same as x_{z01} of the monopole case. Thus the resonant frequency will be the same. The reduced wake force is

$$\hat{F}_{r11} = 4\sqrt{\frac{2\delta(\mu\epsilon - 1)}{\epsilon}}\,. \tag{5.20}$$

Again comparing Eq. (5.16) with the transverse wake of a parallel resonance, the transverse impedance can be inferred. At low frequencies, it can be written as

$$Z_1^{\perp} = -i\frac{Z_0 cL}{2\pi d^3 \omega_{r11}}\hat{F}_{r11} = -i\frac{Z_0 L\delta}{\pi d^2}\left(\mu - \frac{1}{\epsilon}\right)\,. \tag{5.21}$$

Again the contribution of ϵ is negligible when $\mu\epsilon \gg 1$. For the example given in the last section, to cancel the longitudinal space-charge force evolving from the longitudinal space-charge impedance of $|Z_0^{\parallel}/n|_{\rm spch} = 92.11$ Ohms, a 52.96 cm length of ferrite with $\mu = 1000$ is necessary. This ferrite insertion will create a transverse impedance of $-i1.64$ MOhms/m. Note that this is much larger than and over-cancel the transverse space-charge impedance listed in Eq. (3.5) by a factor of more than 2.

VI. PERPENDICULAR BIAS AT SATURATION

When the beam is ramped from the kinetic energy of 1 GeV at injection in the first ring to the kinetic energy of 4.5 GeV at extraction, the space charge impedance will be reduced by a factor of 8.862. We would like the inductance of the ferrite insertion to decrease by the same factor during the ramp. This can be accomplished by passing a dc bias field through the ferrite. To reduce loss, we suggest that the bias field should be perpendicular to the ac magnetic field generated by the beam particles. This dc biased field can be easily provided by placing a solenoid outside the ferrite cylinder.

One way is to set the dc biased field H_c in the beam- or z-direction so high that the magnetization $\vec{M}$ inside the ferrite is saturated and becomes M_s in the same direction. The ac field $\vec{H}_1$ from beam particles is in the transverse or x-y plane. This will produce an ac magnetization $\vec{M}_1$ which precesses about H_c at the gyromagnetic circular frequency of $\omega_c = \gamma H_c$ where $\gamma = 2\pi \times 2.80$ MHz/Oersted. This precession creates an ac magnetization $\vec{M}_1$ in the transverse plane. Since the ferrite is at saturation, there will not be any hysteresis loss. Thus, we have

$$\vec{H} = \hat{z}H_c + \vec{H}_1\,, \qquad \vec{M} = \hat{z}M_s + \vec{M}_1\,. \tag{6.1}$$

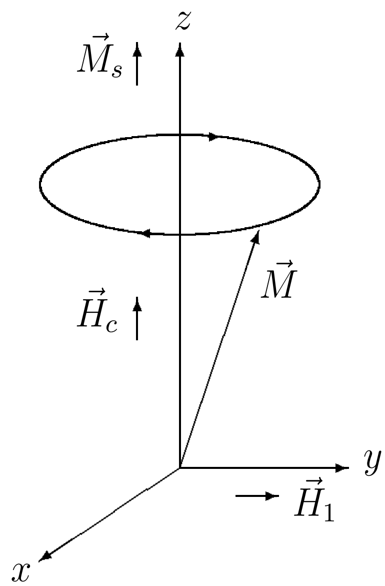

Figure 2: Schematic drawing of system with saturated perpendicular bias H_c in the z direction. With the application of the ac field $\vec{H}_1$ in the y direction, the magnetization $\vec{M}$ acquires an ac component in the x-y plane precessing about the z-axis.

The dc biased field is very much larger than the ac field from the beam, or $|\vec{H}_1| \ll H_c$. The system is represented schematically in Fig. 2. The equation of motion is then approximately

$$\frac{d\vec{M}}{dt} = \gamma(\hat{z}M_s \times \vec{H}_1 + \hat{z}\vec{M} \times H_c)\,. \tag{6.2}$$

Defining the reversible magnetic susceptibility tensor $\overleftrightarrow{\chi}_r$ as $\vec{M}_1 = \overleftrightarrow{\chi}_r \vec{H}_1$, the stationary solution of Eq. (6.2) is

$$\overleftrightarrow{\chi}_r = \begin{pmatrix} \chi & -j\kappa & 0 \\ j\kappa & \chi & 0 \\ 0 & 0 & 1 \end{pmatrix}\,, \tag{6.3}$$

where

$$\frac{\chi}{\mu_0} = \frac{\omega_c\omega_m}{\omega_c^2 - \omega^2}\,, \qquad \frac{\kappa}{\mu_0} = \frac{\omega\omega_m}{\omega_c^2 - \omega^2}\,, \tag{6.4}$$

and

$$\omega_c = \gamma H_c\,, \qquad \omega_m = \gamma\frac{M_s}{\mu_0}\,, \tag{6.5}$$

with μ_0 being the magnetic permeability of free space. There is a resonance at the gyromagnetic resonant frequency $\omega_c = \gamma H_c$, which is proportional to the dc H_c. This explains why we want H_c to be large so that the resonance effect can be avoided. Then, we obtain from Eqs. (6.4), $\kappa/\chi \approx \omega/\omega_c \ll 1$, implying that the off diagonal elements in $\overleftrightarrow{\chi}_r$ can be neglected.

The merit of this saturated biasing is the low loss, because the ferrite is saturated, there will not be hysteresis loss. The only loss is due to spin-wave propagation which is small. The disadvantage is μ' is usually small at or above saturation. The loss is usually introduced by the factor α through $\omega_c \longrightarrow \omega_c - i\omega\alpha$. Writing $\chi = \chi' + \chi''$, the first equation of Eq. (6.4) becomes

$$\frac{\chi'}{\mu_0} = \frac{\left(\frac{\omega_m}{\omega}\right)\left(\frac{\omega_c}{\omega}\right)\left[\left(\frac{\omega_c}{\omega}\right)^2 - 1 + \alpha^2\right]}{\left[\left(\frac{\omega_c}{\omega}\right)^2 - 1 - \alpha^2\right]^2 + 4\left(\frac{\omega_c}{\omega}\right)^2\alpha^2}, \tag{6.6}$$

$$\frac{\chi''}{\mu_0} = \frac{\left(\frac{\omega_m}{\omega}\right)\alpha\left[\left(\frac{\omega_c}{\omega}\right)^2 + 1 + \alpha^2\right]}{\left[\left(\frac{\omega_c}{\omega}\right)^2 - 1 - \alpha^2\right]^2 + 4\left(\frac{\omega_c}{\omega}\right)^2\alpha^2}. \tag{6.7}$$

Perpendicular bias is mostly applied to a cavity for tuning. The ac field is the field generated by the cavity and ω is the resonant frequency of the cavity. Since tuning range of ω is usually small, ω can be considered almost fixed except very near to the gyromagnetic resonance. Therefore, χ is represented as a function of H_c, and this explains why the above formulas have been written as a function of ω_c/ω. Schematically the plots are shown in Fig. 3.

In our application here, the ac field comes from the beam particles. So ω has the range of the bunch spectrum. For example, with the rms bunch length of 28.9 ns, the bunch frequency $\omega/(2\pi)$ has an rms value of ~ 5.5 MHz. It is therefore more convenient to rewrite Eqs. (6.6) and (6.7) as functions of ω instead with H_c held constant,

$$\chi' = \frac{\left(\dfrac{\omega_m}{\omega_c}\right)\left[1 - (1-\alpha^2)\left(\dfrac{\omega}{\omega_c}\right)^2\right]}{\left[1 - (1+\alpha^2)\left(\dfrac{\omega}{\omega_c}\right)^2\right]^2 + 4\alpha^2\left(\dfrac{\omega}{\omega_c}\right)^2}, \tag{6.8}$$

$$\chi'' = \frac{\alpha\left(\dfrac{\omega_m}{\omega_c}\right)\left(\dfrac{\omega}{\omega_c}\right)\left[1 + (1+\alpha^2)\left(\dfrac{\omega}{\omega_c}\right)^2\right]}{\left[1 - (1+\alpha^2)\left(\dfrac{\omega}{\omega_c}\right)^2\right]^2 + 4\alpha^2\left(\dfrac{\omega}{\omega_c}\right)^2}. \tag{6.9}$$

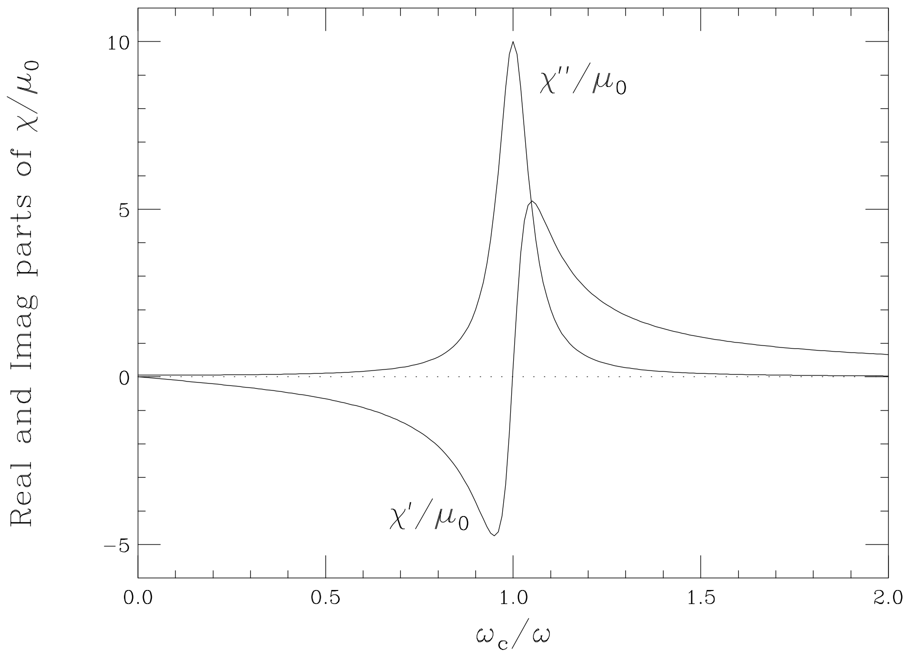

Figure 3: Real and imaginary part of the ferrite susceptibility χ of the ferrite in a cavity as functions the saturated perpendicular biasing field H_c, which is proportional to the gyromagnetic resonant frequency $\omega_c/(2\pi)$. The cavity resonant frequency ω is considered almost constant.

As an example, we choose Ferramic Q-1, which has a saturated flux density $B_s =$ 3300 Gauss at $H_c = 25$ Oersted. Thus, the saturated magnetization is $M_s = 3275$ Gauss. At injection, we bias at $H_c = 25$ Oersted, which gives a resonant frequency of $\omega_c/(2\pi) =$ 70 MHz, which is very much larger than the bunch spectrum spread. We see from Fig. 4 that up to 15 MHz, $\mu' \sim M_s/H_c = 131$. With the ferrite cylinder of inner and outer radii 8 and 10 cm, a length of $L = 2.96$ m is required to cancel $|Z_0^\parallel/n|_{\rm spch} = 92.1$ Ohms. At extraction, μ' must be reduced to $131/8.862 = 14.78$. The biased field should therefore be raised to $H_c = M_s/\mu' = 221.6$ Oersted.

At low frequencies, the loss is

$$\mu'' \longrightarrow \alpha\omega\omega_m/\omega_c^2\,. \tag{6.10}$$

Taking a typical value of $\alpha = 0.05$, we find μ'' varies linearly from 0 and reaches 1.5 at 15 MHz when $H_c = 25$ Oersted at injection. This is illustrated in Fig. 5. At extraction, the loss is reduced by a factor of $8.862^2 = 74.30$ when $H_c = 221.6$ Oersted.

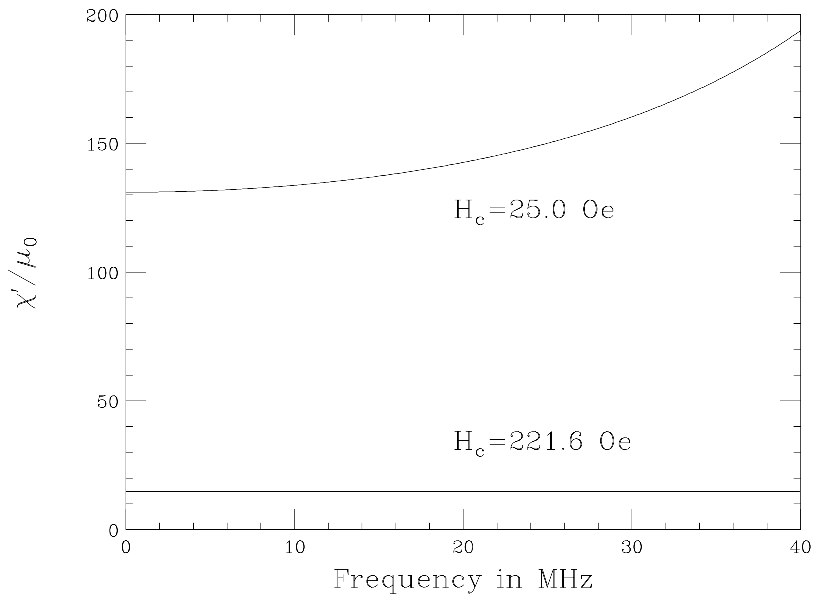

Figure 4: The real part of the ac susceptibility of the ferrite as a function of the beam frequency for the dc bias field 25.0 Oersted at injection and 221.6 Oersted at extraction.

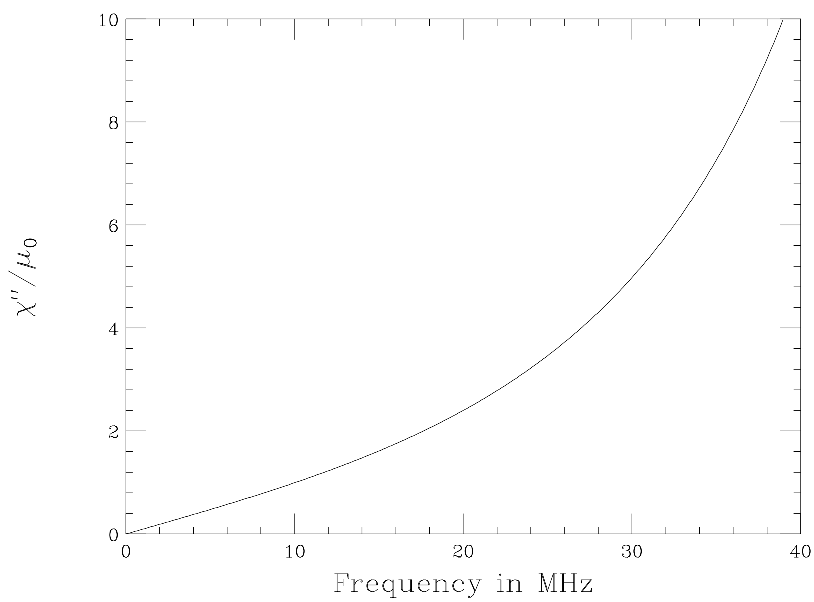

Figure 5: The imaginary part of the ac susceptibility of the ferrite as a function of the beam frequency for the dc bias field of 25.0 Oersted at injection. At extraction with dc bias field of 221.6 Oersted, the imaginary part of the susceptibility is 74.3 times smaller and is too small to be shown in the plot.

VII. CONCLUSION

We have studied the single-bunch instabilities of the two rings of the high-intensity proton driver, and found that the bunches are stable against longitudinal and transverse microwave instabilities. The coupling impedances of both rings are dominated by space charge. The transverse space-charge impedances of both rings are well below their respective instability limits. The longitudinal space-charge impedances are comparable to the longitudinal Keil-Schnell limits. However, since both rings are to be operated below transition, they should be stable.

For the first ring, the space-charge force will modify the rf waveform by very much, and a ferrite insertion is suggested so that the inductance can compensate the space-charge force. In order to control the ferrite induction during ramping, perpendicular biasing at or above saturation is proposed. In this way, the gyromagnetic resonance arriving from large bias field will have a high frequency well above the frequency spread of the particle beam. Also the hysteresis loss in the ferrite can be avoided.

Note added in proof:

On August 2 and 3, an experiment was carried out on the PSR at Los Alamos National Laboratory with an insertion of about 1.5 m ferrite rings in the beam pipe and a solenoid to provide perpendicular biasing in order to control the ferrite permeability. The PSR was running at an intensity of $\sim 3 \times 10^{13}$ protons in one bunch. Preliminary results show that the bunch became longer when the solenoid was switched on. Also the minimum rf voltage to stabilize the bunch was reduced by about 40% when the solenoid was off. The results indicate that the ferrite has been doing the job of counteracting the space space of the bunch and the permeability of the ferrite has been controled successfully by the biased field.

ACKNOWLEDGMENT

The authors would like to thank Drs. J. Griffin and F. Ostiguy for helpful discussions on the properties and applications of ferrite.

References

[1] The $\mu^+\mu^-$ Collider Collaboration, *$\mu^+\mu^-$ Collider: A Feasibility Study*, June 18, 1996, BNL-52503, Fermilab-Conf.-96/092, LBNL-38946.

[2] C. Ankenbrandt, private communication.

[3] J. Laslett, Proc. 1963 Summer Study on Storage Rings, BNL-7534, p.324, 1963.

[4] S. Machida, Proc. 2nd European Particle Accelerator Conf., Nice, France, June 12-16, 1990, ed. P. Marin and P. Mandrillon, p.1655.

[5] C. Ankenbrandt and S. Holmes, Proc. 1987 IEEE Part. Accel. Conf., Washington, DC, 1987, p.1066.

[6] W.C. Weng, private communication.

[7] E. Keil and W. Schnell, CERN Report TH-RF/69-48 (1969); V.K. Neil and A.M. Sessler, Rev. Sci. Instr. **36**, 429 (1965); D. Boussard, CERN Report Lab II/RF/Int./75-2 (1975).

[8] I. Hofmann, Laser and Part. Beams **3**, Part 1, 1 (1985).

[9] A.W. Chao, *Physics of Collective Beam Instabilities in High Energy Accelerators*, Wiley & Sons, 1993, chapter 2.

[10] K.Y. Ng, Phys. Rev. **D42**, 1819 (1990).